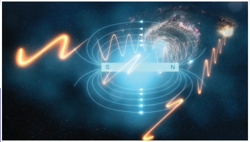

Observations of the (turbulent) Galactic magnetic field

Katia FERRIÈRE

Institut de Recherche en Astrophysique et Planétologie,
Observatoire Midi-Pyrénées, Toulouse, France

Searching for the sources of Galactic cosmic rays

APC, Paris – December 11-14, 2018

Outline

1. Classical methods
   - Dust polarization
   - Faraday rotation
   - Synchrotron emission

2. Faraday tomography

Outline

1. Classical methods
   - Dust polarization
   - Faraday rotation
   - Synchrotron emission
2. Faraday tomography

In a nutshell

- **Polarization of starlight & dust thermal emission**

  Due to *dust grains* $\rightarrow$ general (dusty) ISM

  ☞ $\vec{B}_\perp$ (orientation only)

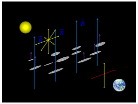

- **Zeeman splitting**

  Molecular & atomic *spectral lines* $\rightarrow$ neutral regions

  ☞ $B_\parallel$ (strength & sign)

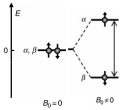

- **Faraday rotation**

  Caused by *thermal electrons* $\rightarrow$ ionized regions

  ☞ $B_\parallel$ (strength & sign)

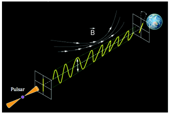

- **Synchrotron emission**

  Produced by *CR electrons* $\rightarrow$ general (CR-filled) ISM

  ☞ $\vec{B}_\perp$ (strength & orientation)

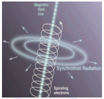

Outline

1. Classical methods
   - Dust polarization
   - Faraday rotation
   - Synchrotron emission
2. Faraday tomography

Polarization direction

- Dust-extinct starlight *(optical)* is polarized $\parallel \vec{B}_\perp$
- Dust thermal emission *(infrared)* is polarized $\perp \vec{B}_\perp$

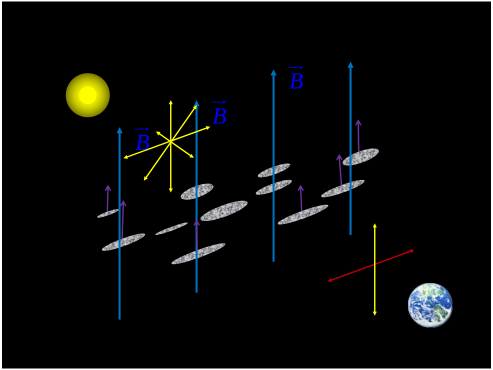

Figure Credit: *Philippe Terral*

Polarization fraction

- Dust-extinct starlight : $p \equiv \frac{P}{I} = \tau \, p_0 \cos^2 \gamma$
- Dust thermal emission : $p \equiv \frac{P}{I} = p_0 \cos^2 \gamma$

$\hookrightarrow p_0 = p_{\max} \, F_{\text{align}} \, F_{\delta B}$

$\vec{B} \in$ POS

$\left(\cos^2 \gamma = 1\right)$

$\Rightarrow p = p_0$

$\vec{B} \perp$ POS

$\left(\cos^2 \gamma = 0\right)$

$\Rightarrow p = 0$

Dust polarization

Altogether

- Polarization *direction* gives *orientation* of $\vec{B}$ *in* POS

- Polarization *fraction* gives *inclination* of $\vec{B}$ *to* POS (for ideal conditions)

Polarization of starlight

$\vec{B}_\perp$ segtors from 8 662 stars

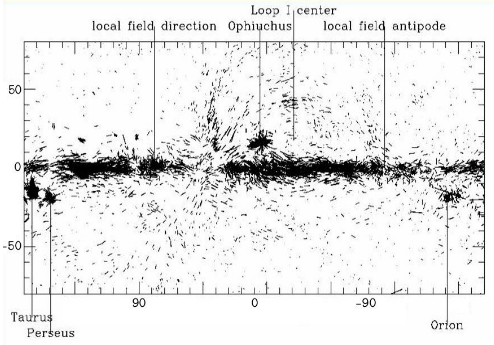

Heiles (2000)

☞ Near the Sun - In disk : $\vec{B}_{\rm ord}$ is horizontal

$\vec{B}_{\rm ord}$ is nearly azimuthal $(p \simeq -7°)$

- In halo : $\vec{B}_{\rm ord}$ has vertical component

Polarization of dust thermal emission

Total intensity & $\vec{B}_\perp$ segtors at 353 GHz

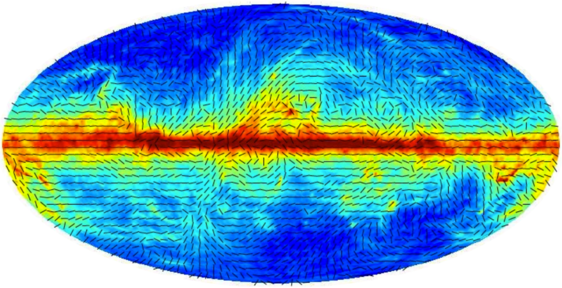

Planck collaboration (2015)

☞ - In disk : $\vec{B}_{\rm ord}$ is horizontal

- In halo : $\vec{B}_{\rm ord}$ has vertical component

Polarization of dust thermal emission

Polarization fraction at 353 GHz

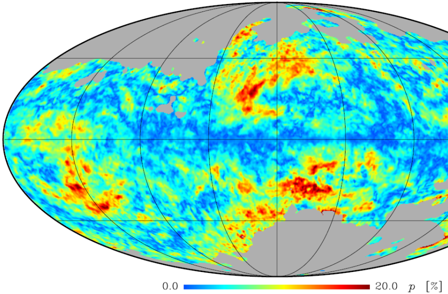

Planck collaboration (2015)

☞ Info on - Inclination of $\vec{B}_{\rm ord}$ to POS : $\cos^2\gamma$

- Magnetic fluctuations : $\frac{B_{\rm fluct}}{B_{\rm ord}}$

- Grain properties & alignment efficiency : $p_{\rm max}$ & $F_{\rm align}$

Polarization of dust thermal emission

Pipe Nebula at 353 GHz

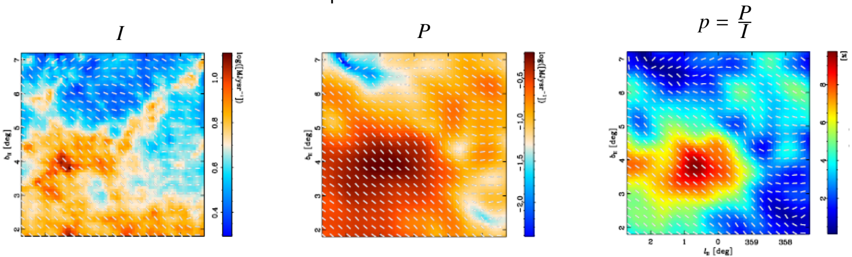

Planck collaboration (2015)

☞ Anti-correlation between $p = \frac{P}{I}$ & $\mathcal{S} = \sqrt{\langle(\Delta\psi)^2\rangle}$

Outline

1. Classical methods
   - Dust polarization
   - Faraday rotation
   - Synchrotron emission

2. Faraday tomography

Rotation measure

$\Delta\theta = \mathrm{RM}\ \lambda^2$ where $\mathrm{RM} = C \int n_e\, B_{\|}\, dl$

☞ $B_{\|}$ in ionized regions

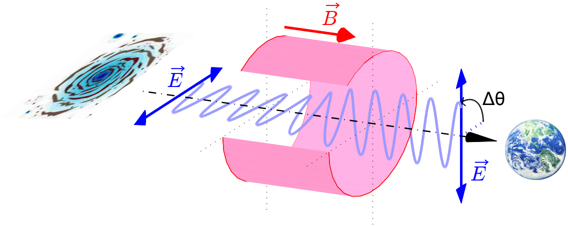

Figure Credit: *Philippe Terral*

Rotation measure

$$\Delta\theta = \mathrm{RM}\ \lambda^2 \quad \text{where} \quad \mathrm{RM} = C \int n_e\, B_{\|}\, dl$$

☞ $B_{\|}$ in ionized regions

RMs of pulsars & EGRSs with $|b| < 8°$

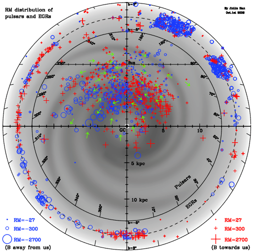

Han (2009)

RMs of EGRSs [NVSS ($\delta > -40°$) + S-PASS ($\delta < 0°$)]

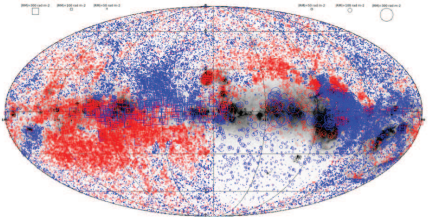

Figure Credit: *Dominic Schnitzeler*

Regular magnetic field

In ionized regions

☞ - $\vec{B}$ has *regular* & *fluctuating* components

Near the Sun : $B_{\rm reg} \simeq 1.5\ \mu$G & $B_{\rm fluct} \sim 5\ \mu$G

- In disk : $\vec{B}_{\rm reg}$ is horizontal & mostly azimuthal

Near the Sun : $\vec{B}_{\rm reg}$ is CW $(p \simeq -8°)$

$\vec{B}_{\rm reg}$ reverses direction with decreasing radius

$\vec{B}_{\rm reg}$ is symmetric in z

- In halo : $\vec{B}_{\rm reg}$ has horizontal & vertical components

$\vec{B}_{\rm reg}$ is CCW at $z > 0$ & CW at $z < 0$

$\rightarrow$ anti-symmetric in z

$(B_{\rm reg})_z \simeq +0.3\ \mu$G toward SGP & $\simeq 0\ \mu$G (?) toward NGP

$\rightarrow$ possibly consistent with sym disk & anti-sym halo

Regular magnetic field

Model of the large-scale magnetic field in the Galactic disk

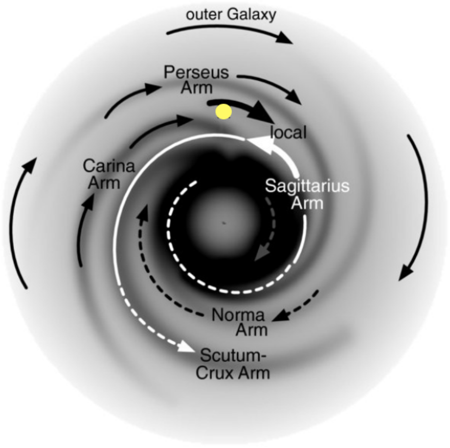

van Eck et al. (2011)

Power spectra: from extragalactic RMs

Combine measured $\mathrm{RM} = C \int n_e \, B_\parallel \, ds$ & $\mathrm{EM} = \int n_e^2 \, ds$

to derive power spectra of δn_e and δB separately *(Minter & Spangler 1996)*

For irregularly spaced sources,

use structure functions $D_\phi(\vec{r}_1 - \vec{r}_2) = \left\langle \left[\delta\phi(\vec{r}_1) - \delta\phi(\vec{r}_2) \right]^2 \right\rangle$

$$D_\phi(\delta\vec{r}) \to P_\phi(\vec{k})$$

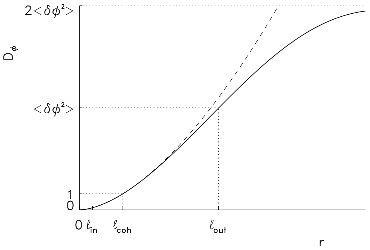

Power spectra: from extragalactic RMs

Combine measured $\mathrm{RM} = C \int n_e B_\parallel \, ds$ & $\mathrm{EM} = \int n_e^2 \, ds$

to derive power spectra of δn_e and δB separately *(Minter & Spangler 1996)*

Structure function of RM

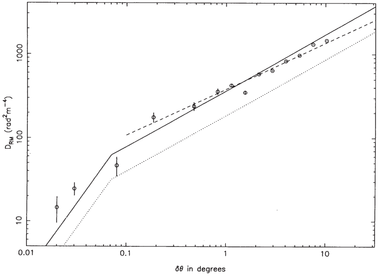

Structure function of EM

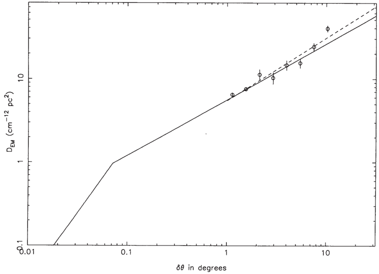

$$D_{\mathrm{RM}} \propto \delta\theta^{\frac{5}{3}} \quad \& \quad D_{\mathrm{EM}} \propto \delta\theta^{\frac{5}{3}} \quad \text{for} \quad \delta\theta < 0.07^\circ$$

$$D_{\mathrm{RM}} \propto \delta\theta^{\frac{2}{3}} \quad \& \quad D_{\mathrm{EM}} \propto \delta\theta^{\frac{2}{3}} \quad \text{for} \quad \delta\theta > 0.07^\circ$$

Power spectra: from extragalactic RMs

Combine measured $\mathrm{RM} = C \int n_\mathrm{e}\, B_\parallel\, ds$ & $\mathrm{EM} = \int n_\mathrm{e}^2\, ds$

to derive power spectra of δn_e and δB separately *(Minter & Spangler 1996)*

$$D_\mathrm{RM} \propto \delta\theta^{\frac{5}{3}} \quad \& \quad D_\mathrm{EM} \propto \delta\theta^{\frac{5}{3}} \qquad \text{for} \quad \delta\theta < 0.07^\circ$$
$$D_\mathrm{RM} \propto \delta\theta^{\frac{2}{3}} \quad \& \quad D_\mathrm{EM} \propto \delta\theta^{\frac{2}{3}} \qquad \text{for} \quad \delta\theta > 0.07^\circ$$

$$\Rightarrow \quad E_n(k) \propto k^{-\frac{5}{3}} \quad \& \quad E_B(k) \propto k^{-\frac{5}{3}} \qquad \text{for} \quad \ell < 3.6 \text{ pc}$$

(assuming $L = 2.9$ kpc)

$$E_n(k) \propto k^{-\frac{2}{3}} \quad \& \quad E_B(k) \propto k^{-\frac{2}{3}} \qquad \text{for} \quad \ell > 3.6 \text{ pc}, \quad \ell < (70 - 100) \text{ pc}$$

☞ - True MHD turbulence

- 3D Kolmogorov for $\ell < 3.6$ pc & 2D for $3.6 \text{ pc} < \ell < (70 - 100)$ pc
- Possibly turbulent sheets of thickness ~ 3.6 pc
- Spectral break at $\ell \simeq 3.6$ pc could explain knee in CR spectrum
  ($\ell \simeq 3.6$ pc corresponds to $E_\perp \simeq 2 \times 10^7$ GeV if $B \simeq 5\ \mu$G)

Power spectra: from extragalactic RMs

Outer scale of RM power spectrum

Structure function of RM

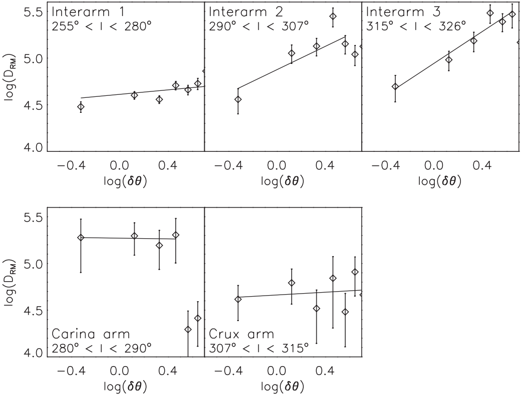

Haverkorn et al. (2008)

- In interarm regions
  - Kolmogorov for $\ell \lesssim 1$ pc
  - Flatter for $\ell \sim (1 - 100)$ pc
  - $\Rightarrow \quad \ell_{\rm out} \sim 100$ pc
- In spiral arms
  - Kolmogorov for $\ell \lesssim 1$ pc
  - Flat for $\ell \gtrsim 1$ pc
  - $\Rightarrow \quad \ell_{\rm out} \sim$ a few pc

Power spectra: from pulsar RMs

Combine measured $\mathrm{RM} = C \int_0^L n_e B_\parallel \, ds$ & $\mathrm{DM} = \int_0^L n_e \, ds$ & L

to derive power spectrum of δB at larges scales *(Han et al. 2004)*

Magnetic energy spectrum

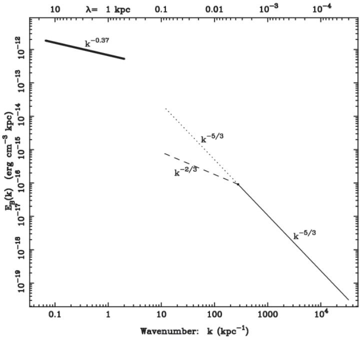

☞ $E_B(k) \propto k^{-0.37}$

for $0.5 \text{ kpc} < \ell < 15 \text{ kpc}$

Fluctuating magnetic field

Strength of fluctuating magnetic field

- From extragalactic RMs
  - $\delta B_{\rm rms} \sim 1~\mu{\rm G}$ for $\ell < 3.6~{\rm pc}$ (Kolmogorov portion) *(Minter & Spangler 1996)*
  - $\delta B_{\rm rms} \gtrsim 1.3~\mu{\rm G}$ *(Gaensler et al. 2001)*
- From Galactic pulsar RMs
  - $\delta B_{\rm rms} \sim 6~\mu{\rm G}$ *(Han et al. 2004)*

Prospects for RM grids

- Pulsars with measured DMs & RMs

  ∗ Currently : 1 133
  (ATNF pulsar catalogue, version 1.58, *Manchester et al. 2005*$^{+}$)

  ∗ Expected with SKA 1 :

  - Total number : ∼ 18 000
  - Density in Galactic plane : ∼ 6 deg^{-2}

  (*Keane et al. 2015*)

- Extragalactic sources with measured RMs

  ∗ Currently : ≃ 42 000
  (*Oppermann et al. 2015*)

  ∗ Expected with SKA 1 :

  - Total number : ∼ $(1 - 4) \times 10^7$
  - Average density : ∼ (300 - 1 000) deg^{-2}

  (*Haverkorn et al. 2015*)

Outline

1. Classical methods
   - Dust polarization
   - Faraday rotation
   - Synchrotron emission

2. Faraday tomography

Total & polarized intensities

$\mathcal{E} = f(\alpha)\, n_{\rm CRe}\, B_\perp^{\,\alpha+1}\, \nu^{-\alpha}$ & $\vec{\mathcal{E}} \perp \vec{B}_\perp$

- **Total intensity** : $I = \int_0^L \mathcal{E}\, ds$ ☞ $B_\perp$ (strength only)
- **Polarized intensity** : $\vec{P} = \int_0^L \vec{\mathcal{E}}\, ds$ ☞ $(\vec{B}_{\rm ord})_\perp$ (strength & orientation)

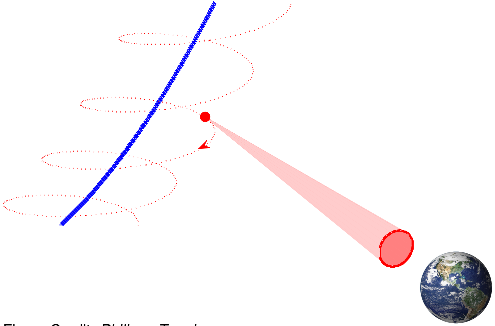

Figure Credit: *Philippe Terral*

Total & polarized intensities

$\mathcal{E} = f(\alpha)\, n_{\rm CRe}\, B_\perp{}^{\alpha+1}\, \nu^{-\alpha}$ & $\vec{\mathcal{E}} \perp \vec{B}_\perp$

- Total intensity : $I = \int_0^L \mathcal{E}\, ds$ ☞ $B_\perp$ (strength only)

- Polarized intensity : $\vec{P} = \int_0^L \vec{\mathcal{E}}\, ds$ ☞ $(\vec{B}_{\rm ord})_\perp$ (strength & orientation)

TI at 1.4 GHz (25m Stockert + 30m Villa Elisa)

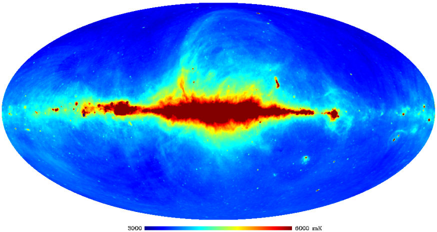

Figure Credit: *Tess Jaffe*

PI at 1.4 GHz (26m DRAO + 30m Villa Elisa)

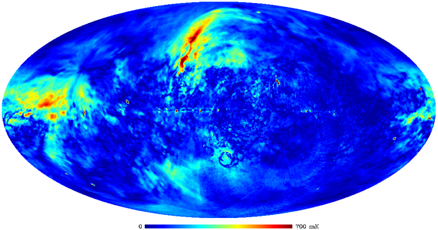

Figure Credit: *Tess Jaffe*

Total & polarized intensities

$$\mathcal{E} = f(\alpha)\, n_{\rm CRe}\, B_\perp^{\,\alpha+1}\, \nu^{-\alpha} \quad \& \quad \vec{\mathcal{E}} \perp \vec{B}_\perp$$

- Total intensity : $I = \int_0^L \mathcal{E}\, ds$ ☞ $B_\perp$ (strength only)
- Polarized intensity : $\vec{P} = \int_0^L \vec{\mathcal{E}}\, ds$ ☞ $(\vec{B}_{\rm ord})_\perp$ (strength & orientation)

TI at 1.4 GHz (25m Stockert + 30m Villa Elisa)

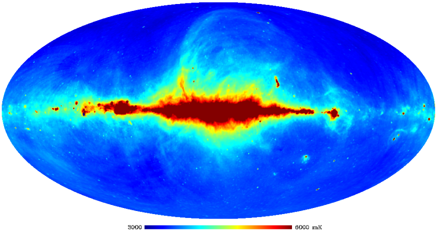

Figure Credit: *Tess Jaffe*

PI & $\vec{B}_\perp$ segtors at 23 GHz (WMAP)

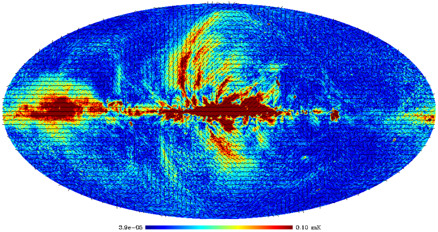

Figure Credit: *Tess Jaffe*

Ordered magnetic field

In general (CR-filled) ISM

☞ - $\vec{B}$ has *ordered* & *fluctuating* components

- Near the Sun : $B_{\rm ord} \sim 3\ \mu$G & $B_{\rm tot} \sim 5\ \mu$G

- Global spatial distribution : $L_{\rm B} \sim 12$ kpc & $H_{\rm B} \sim 4.5$ kpc

- In disk : $\vec{B}_{\rm ord}$ is horizontal
- In halo : $\vec{B}_{\rm ord}$ has horizontal & vertical components

Power spectrum

Angular power spectrum of synchrotron TI toward Fan region

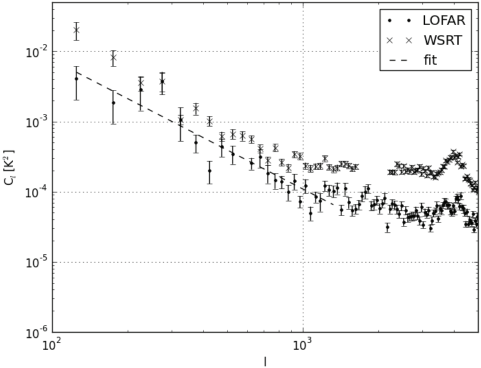

Iacobelli et al. (2013)

☞ $C_l \propto l^{-1.84}$

for $100 < l < 1\,300$

$8' < \delta\theta < 110'$

$\Rightarrow$ $\ell_{\rm out} \sim (10 - 20)$ pc

$\dfrac{B_{\rm ord}}{B_{\rm fluct}} \sim 0.3 - 0.5$

Synchrotron intensity gradients

Synchrotron intensity gradients & $\vec{B}_\perp$ segtors (Planck)

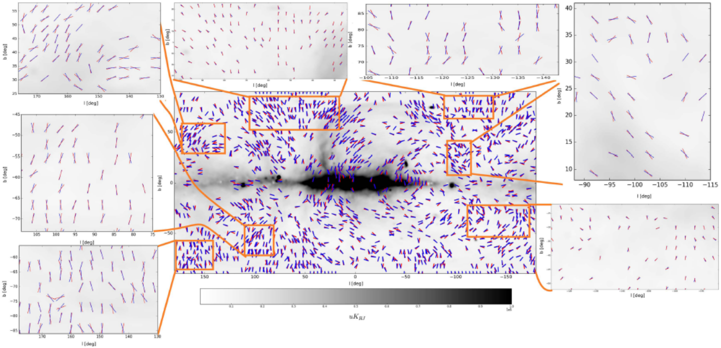

Lazarian et al. (2017)

Synchrotron polarization gradients

TI & PI at 1.4 GHz (ATCA)

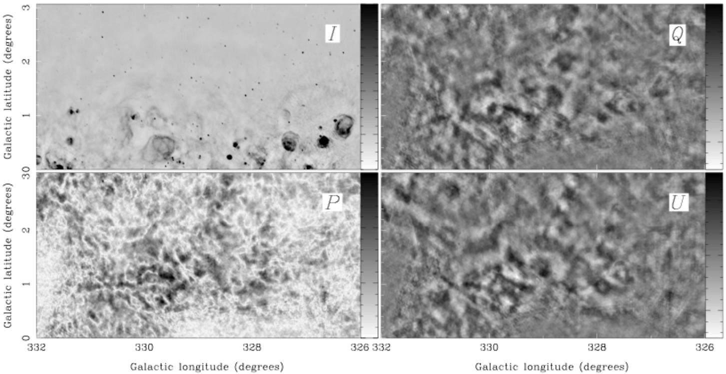

Gaensler et al. (2011)

$$\vec{P} = Q + i\,U$$

Synchrotron polarization gradients

$|\nabla\vec{P}|$ at 1.4 GHz (ATCA)

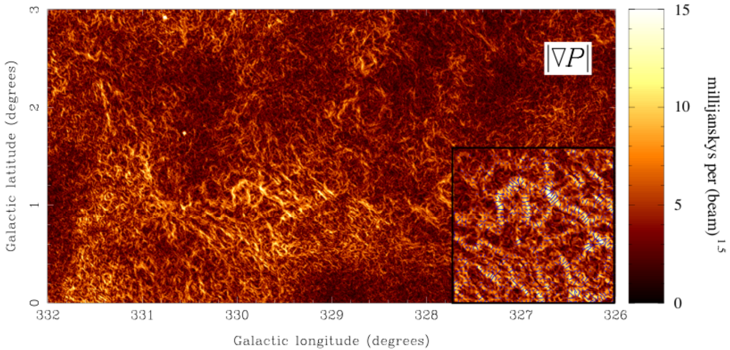

Gaensler et al. (2011)

Comparison with simulations

☞ Interstellar turbulence is subsonic or transsonic *(Burkhart et al. 2012)*

Outline

General concept

- Underlying processes
  - Galactic synchrotron emission : linearly polarized
  - Faraday rotation : λ-dependent
- General idea
  - Measure synchrotron polarized intensity at many different λ
  - Convert λ-dependence into LOS-dependence
- Output

  Faraday cube = 3D cube of synchrotron polarized emission as fc(α, δ, Φ)

General method

- Faraday rotation of background source

$\Theta = \mathrm{RM}\,\lambda^2$ with $\mathrm{RM} = C \int_0^L n_e\, B_{\|}\, ds$ (rotation measure)

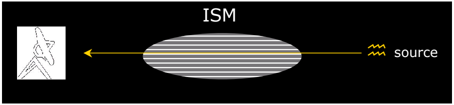

- Faraday rotation of Galactic synchrotron emission

Synchrotron emission & Faraday rotation are *spatially mixed*

$\vec{P}(\lambda^2) = \int \vec{F}(\Phi)\, e^{2i\Phi\lambda^2}\, d\Phi$ with $\Phi(z) = C \int_0^z n_e\, B_{\|}\, ds$ (Faraday depth)

☞ *Fourier transform* of polarized intensity : $\vec{P}(\lambda^2) \rightarrow \vec{F}(\Phi)$

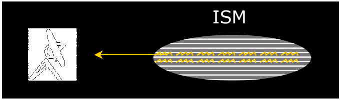

Figure Credit: *Marijke Haverkorn*

Faraday spectrum

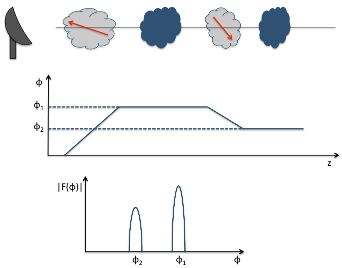

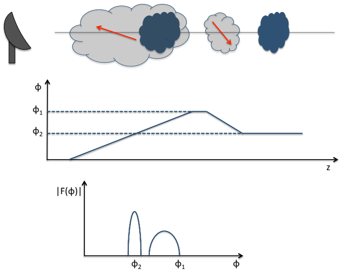

Figure Credit: *Marta Alves*

 = Faraday-rotating cloud

 = synchrotron-emitting cloud

Faraday cube

For given sky area

- Derive *Faraday spectrum*, $\vec{F}(\Phi)$, in many directions (α, δ)
- Combine all derived Faraday spectra into *Faraday cube* = 3D cube of $\vec{F}(\alpha, \delta, \Phi)$

Faraday cube toward Fan region, obtained with LOFAR *(van Eck et al. 2017)*

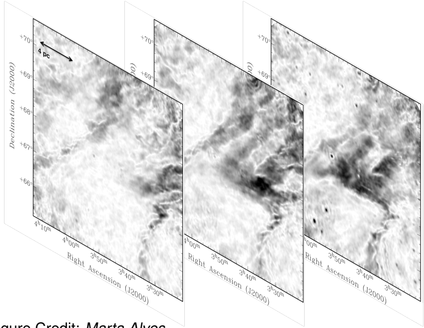

3 slices at

$$\Phi_1 = -2.0 \text{ rad m}^{-2}$$
$$\Phi_2 = -1.5 \text{ rad m}^{-2}$$
$$\Phi_3 = -1.0 \text{ rad m}^{-2}$$

Figure Credit: *Marta Alves*

Extracted information

- From Faraday space to physical space

  - Uncover synchrotron-emitting & Faraday-rotating features in Faraday cube

  - Identify these features with interstellar matter structures

- For synchrotron-emitting regions

  $\int \vec{F}(\Phi)\, d\Phi \quad \Rightarrow \quad \vec{B}_{\perp}$

- For Faraday-rotating regions

  $\Delta\Phi \quad \Rightarrow \quad B_{\|}$

Example of a nearby magnetized bubble

Polarized intensity at 3 different Faraday depths

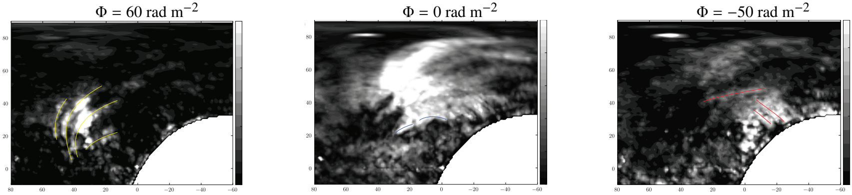

Wolleben et al. (2010)

Interpretation

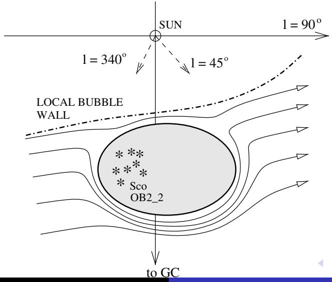

Example of a nearby magnetized bubble

Polarized intensity at 3 different Faraday depths

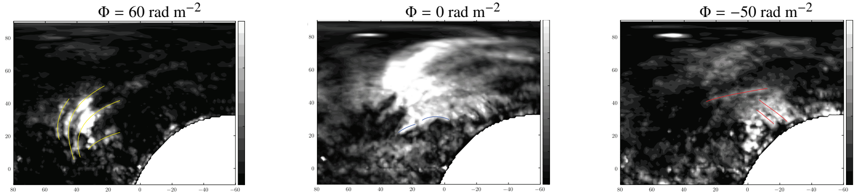

Wolleben et al. (2010)

Interpretation